Evaluation of Multi-band Carrier-less Amplitude and Phase Modulation Performance for VLC under Various Pulse Shaping Filter Parameters

Petr Chvojka[1], Paul Anthony Haigh[2], Stanislav Zvanovec[1], Petr Pesek[1] and Zabih Ghassemlooy[3]

[1]Department of Electromagnetic Field, Faculty of Electrical Engineering, Czech Technical University in Prague,
Technicka 2, 16627, Prague, Czech Republic
[2]High Performance Research Group, Faculty of Engineering, University of Bristol, BS8 1TH, Bristol, U.K.
[3]Optical Communications Research Group, NCRLab, Faculty of Engineering and Environment, Northumbria University,
NE1 8ST, Newcastle upon Tyne, U.K.

Abstract: In multi-band carrier-less amplitude and phase modulation (*m*-CAP), the transmitter and receiver pulse shaping filters have a significant impact on the signal performance. Since *m*-CAP is an emerging and promising modulation format for visible light communications (VLC), it is necessary to balance the system performance and the filter length, due to limited integration density in field programmable gate arrays (FPGAs). In this paper we investigate the *m*-CAP VLC system performance for different number of sub-bands $m = \{2, 5, 10\}$ under varying finite impulse response (FIR) filter parameters, such as the filter length L_f and the roll-off factor β. We show that increasing both β and L_f improves the bit error rate (BER) performance of the system substantially. We demonstrate that a BER target of 10^{-4} is achieved using $L_f \leq 12$ symbols for $m = 5$ and 10 for low order subcarriers. Moreover, the BER limit is attained for $\beta = 0.2$ by all subcarriers, except the last two for $m = 5$ and 10, which is a significant improvement, even considering the slightly increased excess bandwidth in comparison to the literature.

1 INTRODUCTION

As the number of end user devices connected to the internet will increase, the demand for high speed internet connection and the transmission capacity required will grow exponentially (Zvanovec et al., 2015). Thus, the next generation networks (5G) face several challenges such as high spectral and energy efficiency and high capacity. Visible light communications (VLC) is an emerging technology, which is able to meet the mentioned requirements by utilizing existing solid state lighting (SSL) structures based on light-emitting diodes (LEDs). VLC provides users with both illumination and data transmission at the same time and could be used for localization as well (Armstrong et al., 2013).

Despite the advantage in using existing SSL infrastructures, the bottleneck of the VLC system is introduced by LEDs behaving as a first order low pass filter (LPF), with a 3 dB cut-off frequency in the MHz region (Haigh et al., 2014). Thus, spectrally efficient modulation formats such as orthogonal frequency division multiplexing (OFDM) are frequently proposed due to such bandwidth limitations in conjunction with high capacity requirements. OFDM supports bit- and power-allocation algorithms that assign bits and electrical power to each subcarrier (Bykhovsky et al., 2014). However, OFDM suffers from a high peak-to-average power ratio (PAPR) that can lead to signal clipping, due to the LED nonlinear electro-optic characteristic resulting in the link performance degradation (Mesleh et al., 2012).

Recently, the research community has turned attention to carrier-less amplitude and phase (CAP) modulation format as an alternative to OFDM (Wu et al., 2012; Wei et al., 2012; Wu et al., 2013). CAP is similar to quadrature amplitude modulation (QAM). The main difference is that CAP uses finite impulse response (FIR) filters to generate carrier frequencies unlike QAM, which utilizes a local oscillator. This results in a simpler solution for CAP receivers, since time-reversed matched filters are deployed. In previous research it was experimentally shown that CAP outperforms OFDM in VLC when using the sa-
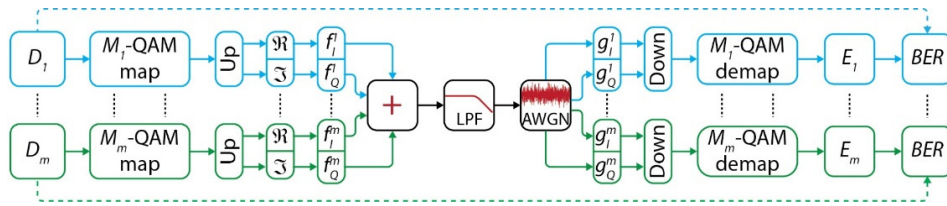
Figure 1: Schematic diagram of the VLC system. Note, that 'UP' and 'DOWN' block represent upsampling and downsampling, respectively.

me experimental setup. The improvement in achieved transmission speed was ∼ 22%, which is significant (Wu et al., 2013). Nevertheless, CAP requires a flat channel frequency response, which is a rare commodity in VLC networks, due to the LEDs LPF behaviour. To overcome this, a new approach called multi-band CAP (*m*-CAP) was proposed for short range optical fibre links (Olmedo et al., 2014). The available bandwidth was split into 6 sub-bands (or subcarriers for compatibility with OFDM nomenclature) and a 6-CAP system was compared to the traditional single CAP (1-CAP) system. Splitting the bandwidth into *m* sub-bands has two key advantages over 1-CAP: *i)* relaxing the flat frequency response requirement and *ii)* allowing to adjust number of bits-per-symbol for each sub-band. Only a slight improvement in data rate (100 Gb/s and 102.4 Gb/s for 1-CAP and 6-CAP, respectively) was shown in (Olmedo et al., 2014), however *m*-CAP outperformed the conventional 1-CAP system in bandwidth efficiency and dispersion.

Thus, we adopted *m*-CAP modulation for VLC systems in our previous work both experimentally (Haigh et al., 2015; Haigh et al., 2015) and theoretically using numerical simulations (Haigh et al., 2015; Werfli et al., 2015; Haigh et al., 2015). For instance, in (Haigh et al., 2015) we showed that for a higher number of sub-bands, a higher transmission capacity can be supported. The highest data rate we achieved was ∼ 31.5 Mb/s in the 10-CAP system, using an LED with a low 4.5 MHz modulation bandwidth. Increasing the number of sub-bands results in a lower bandwidth occupied by each subcarrier. Thus, they are less prone to the frequency dependent attenuation caused by the first order LPF behaviour of an LED and hence can support higher throughput, as mentioned. A highly bandlimited VLC link was investigated in (Haigh et al., 2015). The LPF cut-off frequency was set to 0.1 of the signal bandwidth and it was shown, that 10-CAP system can support up to 40% improvement in the bit rate compared to the traditional 1-CAP for the same bit error rate (BER) target.

As mentioned before, the carrier frequencies are generated by FIR filters, which are crucial in determining the system performance and complexity. Thus, in this paper we investigate performance of the *m*-CAP system using different filter parameters such as filter length L_f and roll-off factor β through numerical simulations. We show that a 2-CAP system does not meet the BER target for any filter length, while usage of filter lengths in the range of $8 < L_f < 12$ is sufficient for the most of the subcarriers except two highest for $m = 5$ and 10. Moreover, just a slight increment of the roll-off factor β results in significant improvement in BER performance when a higher number of sub-bands is deployed. The rest of the paper is organized as follows: in Section 2 the main principles of *m*-CAP and filter parameters are discussed. In Section 3 and 4 the results from *m*-CAP filter analyses are given and the conclusions are drawn, respectively.

2 SYSTEM DESCRIPTION

2.1 Multi-band CAP Principle

The schematic block diagram of the tested system is illustrated in Fig. 1. Firstly, *m* independent data streams of the length of 10^6 are generated. The data is mapped into *M*-QAM constellation symbols, upsampled by means of zero padding and split into the real (in-phase) and imaginary (quadrature) branches. The order of QAM modulation *M* is set to 16 to stay in consistency with recent literature (Haigh et al., 2015). The upsampling factor is given as (Olmedo et al., 2014):

$$n_s = \lceil 2m(1 + \beta) \rceil \qquad (1)$$

where $\lceil \cdot \rceil$ is the ceiling function and β is the roll-off factor of a square root raised cosine (SRRC) filter. The real and imaginary parts of the signal are then passed through the in-phase and quadrature SRRC filters, respectively. The setting of FIR filters will be discussed in detail later with respect to particular parameters under investigation. Finally, the filter outputs are summed up and modulate the LED intensity. The output signal is described by (Haigh et al., 2015; Junwen et al., 2013):

$$s(t) = \sum_{n=1}^{m} \left(s_I^n(t) \otimes f_I^n(t) - s_Q^n(t) \otimes f_Q^n(t) \right) \quad (2)$$

where s_I and s_Q are the real and imaginary QAM symbols for the nth subcarrier and f_I and f_Q are the in-phase and quadrature transmit filter impulse responses, respectively, and $\otimes$ denotes time-domain convolution.

The output signal is passed through an ideal analogue LPF channel and the signal bandwidth is set to $B = 1$ Hz without any loss of generality. Thus, we can expect the same results for any signal bandwidth. The cut-off frequency of the LED is set as $f_c = 0.5$ Hz as in (Haigh et al., 2015), which results in an out of band transmission, where the signal attenuation of 20 dB/decade is assumed. After passing the zero-mean additive white Gaussian noise (AWGN) channel, the signal is passed through time reversed real and imaginary receiver filters, which are matched to the transmit filters. Next, both the real and imaginary parts of the signal are downsampled according to n_s and de-mapped for QAM constellation symbols estimation. Finally, the transmitted bits are compared with the received bits for BER estimation.

As in our previous work we set the BER target limit to 10^{-4} (Haigh et al., 2015), which is below the International Telecommunication Union's (ITU's) recommendation error floor (3.8×10^{-3}) for forward error correction (FEC) with an overhead of 7%.

2.2 FIR Filters

The FIR filters at both the transmitter and receiver are critical for the final m-CAP VLC system performance, since their number is scaled by a factor of $2m$ (two filters for each sub-band placed at both transmitter and receiver). Thus, one must consider the trade-off between performance and system complexity when implementing m-CAP in e.g. field programmable gate array (FPGA). However, to the best of author's knowledge filter parameters for m-CAP VLC systems have never been tested. There is a strong requirement to test such filter performance, as the computational complexity of the FIR filters increases with $2L_f$/symbol.

The pulse shaping SRRC filters have two key parameters: $i)$ roll-off factor β and $ii)$ filter length L_f. The value of β varies in the range of $0 \leq \beta \leq 1$ and determines the excess of bandwidth. A larger β results in the greater bandwidth requirements (see Fig. 2(a)), which is $(1 + \beta)$ times the symbol rate. Clearly, using $\beta = 0$ means ideal spectrum utilization. The impulse responses of the SRRC filters are orthogonal in the

time domain with a 90° phase shift forming a Hilbert pair. They are generated as the product of a cosine and sine wave with SRRC filter impulse response for the real and imaginary parts of the signal, respectively. Obviously, the cosine/sine wave frequency gives the carrier frequency of each sub-band. The impulse responses of the transmit filters are given by (Haigh et al., 2015; Junwen et al., 2013):

$$f_I^m(t) = \begin{bmatrix} \dfrac{\sin[\gamma(1-\beta)] + 4\beta\frac{t}{T_s}\cos[\gamma\delta]}{\gamma\left[1 - \left(4\beta\frac{t}{T_s}\right)^2\right]} \\ \cdot \cos[\gamma(2m-1)\delta] \end{bmatrix} \quad (3)$$

for the in-phase filter and

$$f_Q^m(t) = \begin{bmatrix} \dfrac{\sin[\gamma(1-\beta)] + 4\beta\frac{t}{T_s}\cos[\gamma\delta]}{\gamma\left[1 - \left(4\beta\frac{t}{T_s}\right)^2\right]} \\ \cdot \sin[\gamma(2m-1)\delta] \end{bmatrix} \quad (4)$$

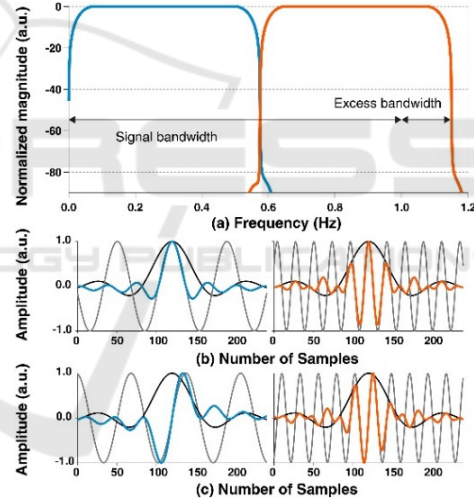for the quadrature filter, where T_s is the symbol duration, $\gamma = \pi t/T_s$ and $\delta = 1+\beta$.

Figure 2: (a) shows frequency responses of the SRRC filters for $m = 2$. The impulse responses for each sub-band for the real and imaginary part of the signal are in Fig. 2(b) and 2(c), respectively. Note the excess bandwidth for $\beta = 0.15$.

Fig. 2(a) illustrates filters' frequency responses for 2-CAP system for each sub-band, the time domain equivalents for the real and imaginary signal are depicted in their respective colours in Fig. 2(b) and 2(c), respectively.

3 RESULTS

In this paper, we investigate the m-CAP VLC system

performance under various filters parameters for the first time. The order of QAM modulation format is set to $M = 16$, while the number of sub-bands is $m = \{2, 5, 10\}$. As mentioned before, the signal bandwidth B and the LED 3-dB modulation bandwidth f_c are 1 Hz and 0.5 Hz, respectively.

We adopted two different approaches and set the parameters to stay in consistency with recent literature (Olmedo et al., 2014; Haigh et al., 2015; Werfli et al., 2015):

- Fixing the roll-off factor $\beta = 0.15$ and varying the filters length in the range of $2 \leq L_f \leq 16$ symbols

- Fixing the filter length $L_f = 10$ symbols and varying the roll-off factor in the range of $0 \leq \beta \leq 1$

3.1 Fixed Roll-off Factor

The number of filter taps is crucial for the system performance, since the implementation of the m-CAP modulation on a digital signal processor (DSP) such as an FPGA is limited by the available

hardware resources. Dividing the signal bandwidth into $m = 10$ sub-bands requires 20 FIR filters at the transmitter part and a further 20 at the receiver. Thus, we investigate the BER performance of the system (see Fig. 1) for a range of L_f. The results are illustrated in Fig. 3(a)-(c) for $E_b/N_0 = 10$ dB (solid line, unfilled markers) and 20 dB (dashed line, filled markers) for each subcarrier (denoted as s) while β is fixed to 0.15. It can be seen that increasing L_f for low values of E_b/N_0 improves the BER performance by one order of magnitude in the best case for $m = 5$ and 10, while for $m = 2$ the improvement in BER is almost negligible. With higher order subcarriers such a performance enhancement due to the increased filter lengths is considerably reduced. This is caused by the attenuation outside of the modulation bandwidth. On the other hand, when higher E_b/N_0 is employed, the BER target is easily met for low order subcarriers for $m = 5$ ($s = 1, 2, 3$) and 10 ($s = 1, 2, …, 8$). However, note: the 2-CAP system completely fails to meet the BER limit in the whole considered range of L_f due to a wider bandwidth requirement, which is five times higher that of 10-CAP. The performance improvement is further illustrated in Fig. 3(d), where
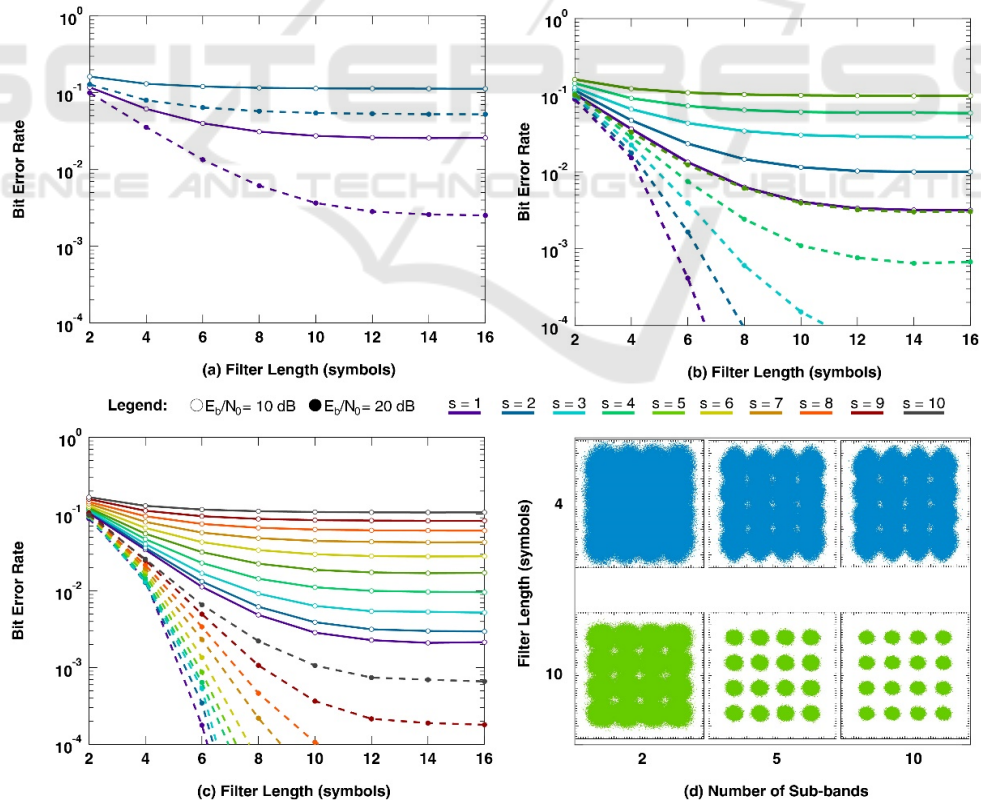

Figure 3: BER performance for a range of L_f for different values of m is shown in (a)-(c). Two different values of $E_b/N_0 = 10$ and 20 dB were considered. The performance improvement is most significant for low order subcarriers for $m = 5$ and 10. When employing $m = 2$, BER target is never met. Received constellation diagrams are shown in Fig. 3(d) for each m for the subcarrier $s = 1$ and two filter lengths $L_f = 4$ and 10 at $E_b/N_0 = 20$ dB.

constellation diagrams for the subcarrier $s = 1$ for each value of m and filter lengths $L_f = 4$ and 10 are illustrated.
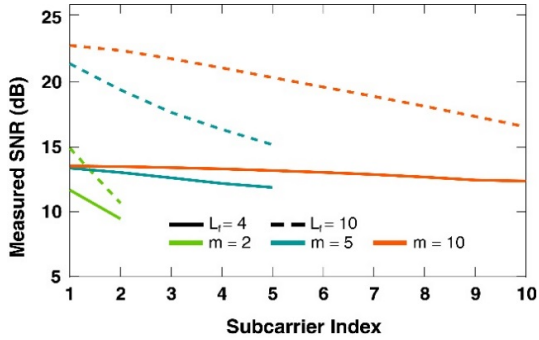

Figure 4: The measured SNR for each subcarrier for a range of m and $L_f = 4$ and 10 at $E_b/N_0 = 20$ dB. Increasing the number of subcarriers increases the differences between measured SNR when using short (4 symbols) and long (10 symbols) filter.

The highest value of L_f to attain the BER target is 12, which is reflected in Fig. 3(b) and 3(c) for $s = 3$ and 8, respectively. This introduces an important

result: utilization of longer filters (i.e., $L_f > 12$) for higher order subcarriers is impractical since no additional BER improvement is achieved. Fig. 4 illustrates the measured signal-to-noise (SNR) ratio for the range of $m = \{2, 5, 10\}$ for $L_f = 4$ (solid line) and 10 (dashed line) at $E_b/N_0 = 20$ dB. By utilization of higher order m-CAP system we can experience increasing SNR gain when compared short and long filter. The SNR gain for the last subcarrier is then ~ 1.2 dB, ~ 3.3 dB and ~ 4.1 dB for $m = 2$, 5 and 10, respectively.

3.2 Fixed Filter Length

The roll-off factor β determines the excess of bandwidth, as mentioned. Thus, using lower values of β is appropriate to save the bandwidth employed in the system. In contrast, it is also possible to increase the system BER performance at the cost of the bandwidth.

Fig. 5(a)-(c) illustrate the BER performance of the system for a range of β for all values of m under E_b/N_0 of 10 dB (solid line, unfilled markers) and 20 dB (dashed line, filled markers) and for $L_f = 10$.
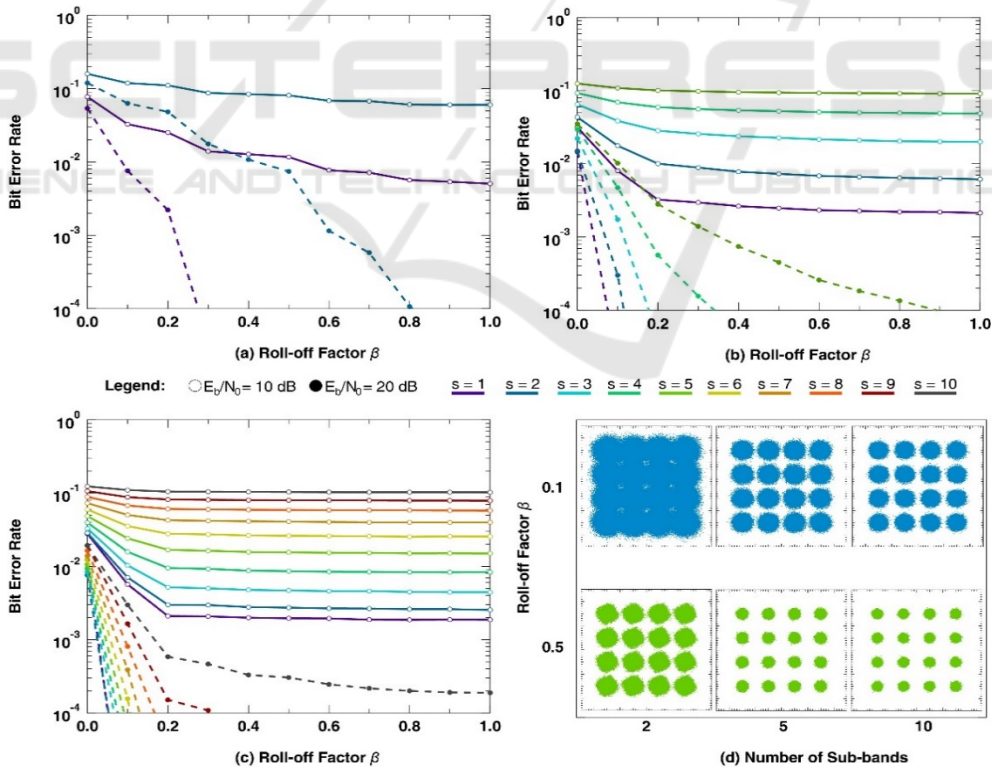

Figure 5: BER performance for a range of β for each m is shown in (a)-(c). Two different values of $E_b/N_0 = 10$ and 20 dB were considered. Only slight increment of β improves the BER performance for low order subcarriers for $m = 5$ and 10. When employing $m = 2$, BER target is met for $\beta = 0.3$ and 0.8 for the subcarriers $s = 1$ and $s = 2$, respectively. Received constellation diagrams are shown in Fig. 5(d) for each m for the subcarrier $s = 1$ and two values of $\beta = 0.1$ and 0.5 at $E_b/N_0 = 20$ dB showing improved performance while increasing β.

The results show that the performance enhancement of each subcarrier is negligible with increasing β at $E_b/N_0 = 10$ dB (maximum one order of magnitude for low order subcarriers for $m = 5$ and 10). Surprisingly, setting $\beta > 0.2$ does not bring any additional improvement and BER curves have almost constant character for $m = 5$ and 10.

On the other hand, only a slight increment of β improves the BER performance significantly for lower order subcarriers at higher E_b/N_0 (i.e., 20 dB). The BER target is achieved by almost all subcarriers, except the last subcarriers, i.e., $s = 4$, 5 and for $m = 5$ and $s = 8$, 9 for $m = 10$, respectively, for $\beta = 0.2$. This is remarkable improvement when compared to E_b/N_0 of 10 dB even in the cost of a slightly increased bandwidth excess. Moreover, both subcarriers in the 2-CAP system attain to meet the BER target when using $\beta = 0.3$ and 0.8 for $s = 1$ and 2, respectively. This is in contrast with Fig. 3(a) where both subcarriers failed to achieve the BER target even for longer FIR filters. Fig. 5(d) illustrates received constellation diagrams for $s = 1$ for each value of $m = \{2, 5, 10\}$ and $\beta = 0.1$ and 0.5 showing the performance improvement while increasing β.

The measured SNR for each subcarrier for the range of m for $\beta = 0.1$ (dashed line) and 0.5 (solid line) at $E_b/N_0 = 20$ dB is illustrated in Fig. 6. It is clear that the SNR gain for $\beta = 0.5$ is decreased when the higher order subcarriers are deployed. For instance, the SNR gain for the last subcarrier is ~ 4.5 dB, ~ 3.5 dB and ~ 2 dB for $m = 2$, 5 and 10, respectively, which is in contrast with previous measurements in Fig. 4. This is caused by the higher bandwidth requirements for $\beta = 0.5$, which results in larger attenuation acting on the individual subcarriers.
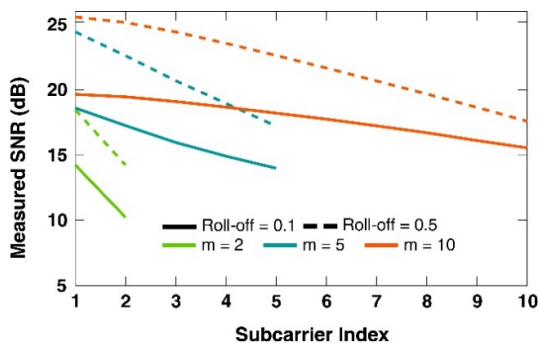

Figure 6: The measured SNR for each subcarrier for a range of m and $\beta = 0.1$ and 0.5 at $E_b/N_0 = 20$ dB. Increasing the number of sub-bands reduces the SNR gain for higher order subcarriers when employing a higher roll-off factor β.

4 CONCLUSIONS

In this paper we investigated the m-CAP performance under varying filter parameters such as filter length and roll-off factor. Increasing both parameters considerably improves the BER performance of the system. The main result for this analyses towards real implementation is that deploying $L_f > 12$ symbols is impractical, since no more performance improvement can be achieved for $m = 5$ and 10. The 2-CAP system utilization is not recommended since it failed to attain BER target for any value of L_f. The roll-off factor β has significant impact on the system performance especially at higher E_b/N_0. The BER target was achieved for the range of values of β for all the subcarriers in the tested system except the highest subcarrier of $m = 10$.

For future work, we will implement m-CAP system in FPGA for further investigation of filters' impact on the system performance for the cases of limited hardware resources.

ACKNOWLEDGEMENTS

REFERENCES

Zvanovec, S., Chvojka, P., Haigh, P.A., Ghasemlooy, Z., Visible light communications towards 5G, *Radioengineering,* vol. 24, April 2015.

Armstrong, J.; Sekercioglu, Y.; Neild, A., Visible light positioning: a roadmap for international standardization, in *Communications Magazine, IEEE*, vol.51, no.12, pp.68-73, December 2013.

Haigh, P. A., Ghassemlooy, Z., Rajbhandari, S., Papakonstantinou, I., Popoola W., Visible Light Communications: 170 Mb/s Using an Artificial Neural Network Equalizer in a Low Bandwidth White Light Configuration, *Lightwave Technology, Journal of,* vol. 32, pp. 1807-1813, 2014.

Bykhovsky, D., Arnon S., An Experimental Comparison of Different Bit-and-Power-Allocation Algorithms for DCO-OFDM, *Lightwave Technology, Journal of,* vol., vol. 32, pp. 1559-1564, Apr 15 2014.

Mesleh, R.; Elgala, H.; Haas, H., LED nonlinearity mitigation techniques in optical wireless OFDM communication systems, in *Optical Communications and Networking, IEEE/OSA Journal of* , vol.4, no.11, pp.865-875, Nov. 2012.

Wu, F.M., Lin, C.T., Wei. C.C., Chen, C.W., Huang, H.T., Ho, C.H., 1.1-Gb/s White-LED-Based Visible Light Communication Employing Carrier-Less Amplitude

and Phase Modulation, in *Photonics Technology Letters, IEEE* , vol.24, no.19, pp.1730-1732, Oct.1, 2012.

Wei, J.L., Ingham, J.D., Cunningham, D.G., Penty, R.V., White, I.H., Performance and Power Dissipation Comparisons Between 28 Gb/s NRZ, PAM, CAP and Optical OFDM Systems for Data Communication Applications, in *Lightwave Technology, Journal of* , vol.30, no.20, pp.3273-3280, Oct.15, 2012.

Wu, F.M., Lin, C.T., Wei, C.C., Chen, C.W., Chen, Z.Y., Huang, H.T., Sien Chi, Performance Comparison of OFDM Signal and CAP Signal Over High Capacity RGB-LED-Based WDM Visible Light Communication, in *Photonics Journal, IEEE* , vol.5, no.4, pp.7901507-7901507, Aug. 2013.

Olmedo, M.I., Tianjian, Z., Jensen, J.B., Qiwen, Z.,Xiaogeng X., Popov, S., Monroy, I.T., Multiband Carrierless Amplitude Phase Modulation for High Capacity Optical Data Links, in *Lightwave Technology, Journal of* , vol.32, no.4, pp.798-804, Feb.15, 2014.

Haigh, P.A., Burton, A., Werfli, K., Le Minh, H., Bentley, E., Chvojka, P., Popoola, W.O., Papakonstantinou, I., Zvanovec, S., A Multi-CAP Visible-Light Communications System With 4.85-b/s/Hz Spectral Efficiency, in *Selected Areas in Communications, IEEE Journal on* , vol.33, no.9, pp.1771-1779, Sept. 2015.

Haigh, P.A., Chvojka, P., Zvanovec, S., Ghassemlooy, Z., Son T.L., Kanesan, T., Giacoumidis, E., Doran, N.J., Papakonstantinou, I., Darwazeh, I., "Experimental verification of visible light communications based on multi-band CAP modulation," in *Optical Fiber Communications Conference and Exhibition (OFC), 2015* , vol., no., pp.1-3, 22-26 March 2015.

Haigh, P.A., Thai Le. S., Zvanovec, S., Ghassemlooy, Z., Pengfei L., Tongyang X., Chvojka, P., Kanesan, T., Giacoumidis, E., Canyelles-Pericas, P., Minh H.L., Popoola, W., Rajbhandari, S., Papakonstantinou, I., Darwazeh, I., Multi-band carrier-less amplitude and phase modulation for bandlimited visible light communications systems, in *Wireless Communications, IEEE* , vol.22, no.2, pp.46-53, April 2015.

Werfli, K., Haigh, P.A., Ghassemlooy, Z., Chvojka, P., Zvanovec, S., Rajbhandari, S., Long, S., Multi-band carrier-less amplitude and phase modulation with decision feedback equalization for bandlimited VLC systems, in *Optical Wireless Communications (IWOW), 2015 4th International Workshop on* , vol., no., pp.6-10, 7-8 Sept. 2015.

Haigh, P.A., Aguado, A., Ghassemlooy, Z., Chvojka, P., Werfli, K., Zvanovec, S., Ertunc, E., Kanesan, T., Multi-band carrier-less amplitude and phase modulation for highly bandlimited visible light communications — Invited paper, in *Wireless Communications & Signal Processing (WCSP), 2015 International Conference on* , vol., no., pp.1-5, 15-17 Oct. 2015.

Junwen Z., Jianjun Y., Fan L., Nan C., Ze D., Xinying L., 11 × 5 × 9.3Gb/s WDM-CAP-PON based on optical single-side band multi-level multi-band carrier-less

amplitude and phase modulation with direct detection, Opt. Express 21, 18842-18848 (2013).